

## Chemical Abundances in 35 Metal-Poor Stars. I. Basic Data

Jeong-Deok Lee<sup>1,2</sup>, Sang-Gak Lee<sup>2</sup>, & Kang-Min Kim<sup>3</sup>

leejd@astro.snu.ac.kr

## A B S T R A C T

We carried out a homogeneous abundance study for various elements, including  $\alpha$ -elements, iron peak elements and  $n$ -capture elements for 35 metal-poor stars with a wide metallicity range ( $-3.0 \leq [\text{Fe}/\text{H}] \leq -0.5$ ). High-resolution ( $R \sim 30\text{k}$ ), high signal-to-noise ( $S/N \sim 110$ ) spectra with a wavelength range of 3800 to 10500 Å using the Bohyunsan Optical Echelle Spectrograph (BOES). Equivalent widths were measured by means of the Gaussian-fitting method for numerous isolated weak lines of elements. Atmospheric parameters were determined by a self-consistent LTE analysis technique using Fe I and Fe II lines. In this study, we present the EWs of lines and atmospheric parameters for 35 metal-poor stars.

Subject headings: stars: abundance – stars: population II – Galaxy: abundance – Galaxy: evolution

## 1. INTRODUCTION

The abundance patterns of metal-poor stars provide information on the formation, evolution, and supernova explosions of massive stars formed in the early epoch of the Galaxy formation (e.g. Tinsley 1980; Pagel 1997; Matteucci 2001). They also provide important clues for understanding of the early stage of the chemical evolution of the Galaxy. Many high-resolution spectroscopic abundance studies for metal-poor stars have been carried out (e.g. McWilliam et al. 1995; Ryan, Norris, & Beers 1996; Fulbright 2000; Burris et al. 2000; Gratton et al. 2003; Cayrel et al. 2004; Honda et al. 2004; Aoki et al. 2005; Francois et al.

---

<sup>1</sup>Astrophysics Research Center for the Structure and Evolution of the Cosmos (ARCSEC), Sejong University, Seoul, 143-747, South Korea

<sup>2</sup>Department of Physics and Astronomy, Seoul National University, Seoul 151-742, South Korea

<sup>3</sup>Korea Astronomy & Space Science Institute, 61-1 W haam -dong, Yuseong-gu, Taejeon 305-348, South Korea

2007) and their results have shown that the abundance patterns of metal-poor stars differ from those of the Sun. In particular, it has been established that the ratio of  $\alpha$ -elements to iron ratio in stars with  $[\text{Fe}/\text{H}] < -1.0$  is greater than the solar ratio by  $+0.4$  dex (Weiler, Sneden, & Truran 1989). This indicates the complex nature of the chemical enrichment.

The general explanation for the chemical evolution of the Galaxy has been based on the products of the two main types of supernovae (Tinsley 1980). The first, comprising the Type II SN and Type Ib/Ic SNe which are the core-collapse-induced explosions of massive stars. The second, the Type Ia SN is the thermonuclear explosion of an accreting white dwarf in a close binary system. The core-collapse SNe breakout shortly after early Galaxy formation because their progenitors are massive stars with short lifetimes, while Type Ia SNe occur after completing at least one stellar lifetime of  $10^9$  yr (for an  $8M_{\odot}$  star) resulting in the formation of a white dwarf (Chiosi et al. 1992).  $\alpha$ -elements are the main products of Type II and Type Ib/Ic SNe while Fe is mainly produced by Type Ia SNe. Therefore the ratio of  $\alpha$ -elements to Fe ratio is high in the halo stars that were formed in the early stage of the Galaxy however this ratio reduces to the solar value as observed in the trends of  $\alpha$ -elements along metallicity.

However, the primary nucleosynthetic sources for most elements are not well known. A relative abundance ratio, for instance, the ratio of an element to Fe is a good tool for investigating the product site of each element. However the inhomogeneous abundance results of previous studies, which showed large scatters and/or some shifts, rule out the use of this technique for this purpose. In order to determine the abundance of a given element, the atmospheric parameters (temperature  $T_{\text{eff}}$ , surface gravity  $\log g$ , micro-turbulent velocity  $v_t$ , and overall metallicity represented by  $[\text{Fe}/\text{H}]$ ) need to be derived. Therefore differences in these parameters result in differences in the results of abundance analysis. The choice of the lines used for analysis and the oscillator strength value ( $\log gf$ ) adopted for deriving the abundance also results in uncertainties and systematic differences in the abundance results. A single-line approximation is found to be inadequate for some spectral lines of odd atomic number elements with significant hyperfine structures Ryan, Norris, & Beers (1996). It has been shown that ignoring the hyperfine structure could lead to abundance errors of up to 0.6 dex. Therefore, we aim to obtain abundances of elements in stars with wide metallicity ranges as accurately as possible by using homogeneous methods.

We divided the elements into three groups, namely, light elements ( $Z \leq 20$ ), iron-peak elements ( $21 \leq Z \leq 30$ ), and  $n$ -capture elements ( $Z \geq 38$ ). Light elements are good tools for judging the surface chemical contamination due to the internal mixing in giants. Iron-peak elements which are mainly produced by explosive Si burning can give important information

on the supernova explosions. The iron-peak elements particularly in metal-poor stars with  $[\text{Fe}/\text{H}] < -1.0$  are produced in massive core-collapse supernovae (Tinsley 1980) and provide important constraints for models of type II SNe.

The n-capture process is responsible for the production of heavy elements beyond the iron-peak elements, however, its site has not yet been determined with certainty. In particular, the nucleosynthesis process of light n-capture elements is proposed to be a combination of various processes (Montes et al. 2007). Further, radioactive elements with sufficiently long half-lives, such as uranium (U,  $Z=92$ ) and thorium (Th,  $Z=90$ ) can provide a constraint on the age of metal-poor stars. In order to determine the age of old stars with unstable radioactive elements, a stable element synthesized in the same event is required to be set as reference.

The transition probabilities of rare-earth n-capture elements and their stable isotopes such as La, Sm, Eu, and Hf have recently been measured with very high accuracy by Lawler and associates (e.g. Den Hartog et al. 2006; Lawler et al. 2001a,b, 2007). This has enabled the derivation of more reliable n-capture element abundance, which may provide new insights on the roles of the n-capture process in the initial burst of Galactic nucleosynthesis.

## 2. Observations and reductions

### 2.1. Observations

We selected the target stars for our study based on the following criteria. Firstly, due to the small aperture (1.8 m) of Bohyunsan Optical Astronomical Observatory (BOAO), we selected stars with a visual magnitude brighter than 10 mag. Secondly, metal-poor stars whose metallicity was determined as  $[\text{Fe}/\text{H}] < -1.0$  by previous spectroscopic studies were selected. Thirdly, stars that are known to have a high proper-motion but do not have previous abundance studies were also included in our target set. We excluded K- and M-type stars that have strong molecular lines as well as metallic lines that are too strong and blended with other lines.

We have obtained high-resolution echelle spectra for 35 metal-poor stars using the Bohyunsan Optical Echelle Spectrograph (BOES) (Kim et al. 2002) in two runs scheduled in November 2005 and April 2006. BOES is a fiber-fed echelle spectrograph mounted on a 1.8-meter telescope at BOAO (Bohyunsan Optical Astronomical Observatory). The BOES detector is an EEV-CCD with  $2048 \times 4102$  pixels and a pixel size of  $15 \mu\text{m}$ . The BOES covers a wide wavelength range (3800 to 10500 Å) in a single exposure and has a high efficiency ( $\sim 15\%$ ). There are three kinds of fiber sets, with apertures of 80  $\mu\text{m}$  ( $1:1^{\text{th}}$ ),

200 m ( $2.9''$ ), and 300 m ( $4.2''$ ) corresponding to spectral resolving powers of  $R \approx 90000$ , 44000, and 30000, respectively.

We observed most of the targets with the largest aperture (300 m) in order to minimize light loss and obtain spectra with high signal-to-noise ratio because of the poor weather conditions at BOAO (The seeing condition was  $3''$  in the first run while that on the second run was  $4''$ ) during the observing runs. Six stars (HD 94028, HD 93487, HD 101227, HD 118659, HD 148816, and HD 159482) were observed using an aperture of 200 m ( $2.9''$ ), which gives a better resolution. We observed no significant difference on comparing the spectra observed from different apertures. A resolving power of  $R \approx 30k$  was found to be satisfactory for conducting abundance analysis. We also observed B-type stars on every night to obtain telluric line references.

We obtained bias frames for zero-correction and tungsten-halogen lamp (THL) frames for flat-fielding, and Th-Ar spectra for wavelength calibration. Since dark current of BOES CCD is very small ( $2e^-/\text{hr/pixel}$ ) relative to read-out noise ( $3e^-$ ), it is not necessary to obtain dark frames. The observation log is presented in Table.1

## 2.2. Reductions

The reductions were performed by following the standard steps for echelle spectrum using IRAF. The biases were first corrected by subtracting the median combined bias frame using the IRAF/codred task. The dark currents were not corrected because the dark current of the BOES CCD is negligibly small.

We adapted a technique for aperture extractions and flattening that differs slightly from the standard reduction procedures. We first prepared a master flat image by combining preprocessed flat images. This master flat image is used only as aperture tracing reference. Using this master flat image, we defined apertures and background regions to be used for scattered light subtraction using the IRAF/ECHELLE/apall task. Subsequently, flat spectra and object spectra were extracted. We then produced the master flat spectrum by combining the flat spectra using the IRAF/ECHELLE/scombine task.

The flat-field correction was carried out by dividing each extracted order of the object spectra by the corresponding order of the master flat spectrum. The blaze function is also corrected using this procedure. Since the THL lamp is not a perfect flat source, the flux of the flat-corrected spectra becomes distorted, however this distortion can be corrected by continuum normalization. Compared to the standard echelle reduction procedure, this procedure is faster and simple and it corrects the blaze function prior to the continuum

normalization. For the case wherein the information of the flux is not required and only the continuum-normalized spectrum is needed (usually for equivalent width (EW) measurements) this procedure would be more efficient for the reduction process.

The wavelength calibration function was obtained using the IRAF/ECHELLE/identify task based on the Th-Ar lamp spectrum corresponding to the first night of the observing run. The daily variation in the wavelength of BOES was very small ( $< 0.001 \text{ \AA}$ ), therefore, the IRAF/ECHELLE/identify task was utilized for the remaining nights of the run. Figure 1 shows a small section of the sample spectra around the H $\gamma$  line, with a wavelength range of 4320 to 4350  $\text{\AA}$  for seven stars whose metallicities  $[\text{Fe}/\text{H}]$  range from  $-0.63$  to  $-2.26$  dex.

### 2.3. Equivalent Widths

Equivalent widths for most elements were measured using Gaussian fitting in the IRAF/splot task. Local continuum was defined by visual inspection for each line. Weak Fe I and Fe II lines with  $\log(\text{EW} / \text{\AA}) < -4.9$  or EWs less than 100 m $\text{\AA}$  were used to determine the atmospheric parameters and to carry out abundance analysis, as strong lines lie in the over-saturation region of the curve of growth, where Gaussian fitting is inadequate and an accurate damping constant is required. However, when only strong lines were available for abundance analysis, we measured EWs by means of Voigt profile fitting. The sources of adopted atomic information are listed in Table 3. A small sample of measured equivalent widths, along with the corresponding atomic information, is presented in Table 2.

We compared the measured EWs with those of previous studies. A graphical comparison for the common stars is shown in Figure. 2 and Figure. 3. Four stars, namely, BD + 29 366, HD 19445, HD 64090, and HD 84937 are common between our study and Gratton et al. (2003). The mean differences (this work minus Gratton et al. (2003)) are  $0.50 \pm 0.23$  m $\text{\AA}$  (sdom<sup>1</sup>, 320 lines) for BD + 29 366,  $0.03 \pm 0.29$  m $\text{\AA}$  (110 lines) for HD 19445,  $0.46 \pm 0.46$  m $\text{\AA}$  (96 lines) for HD 64090, and  $1.36 \pm 0.57$  m $\text{\AA}$  (20 lines) for HD 84937. Figure. 3 shows the comparison of EWs of HD 122563 with those of Cayrel et al. (2004) and Honda et al. (2004). The mean differences corresponding to Cayrel et al. (2004) and Honda et al. (2004) are  $0.25 \pm 0.27$  m $\text{\AA}$  (78 lines) and  $0.33 \pm 0.18$  m $\text{\AA}$  (67 lines), respectively. There is no significant offset observed in the measurement of EWs.

The expected EW uncertainty derived from Cayrel's formula (1988) for our spectra with  $S/N \approx 200$  is  $\approx 2$  m $\text{\AA}$ . This uncertainty ignores the measurement errors that occur in

---

<sup>1</sup>sdom, standard deviation of mean =  $\frac{\sigma}{\sqrt{N}}$

continuum definition and result from the departure of the Gaussian profile of the observed line. For weak lines, the departure from Gaussian line profile is negligible, while the major error in EW measurements results from the local continuum definition. We repeated the EW measurements for some well isolated lines by setting different local continuum to obtain an error of less than 4 mÅ, however, we found that the error in EW depends on the line strength and signal-to-noise ratio of a spectrum.

## 2.4. Radial Velocities

Radial velocities were measured from the observed centers of the Fe I and Fe II lines that are well-isolated and have well-defined Gaussian profiles. The distribution of radial velocities derived from each line for a star was Gaussian-fitted to obtain the stellar velocity, as Figure. 4(a). The radial velocities for program stars are presented in the last column of Table. 4. The typical error of radial velocity (2 dispersion in the Gaussian profile) is 0.45 km/s. A comparison of the radial velocities obtained in this work and those of previous studies (Nordstrom et al. 2004; Latham et al. 2002) is presented in Figure. 4(b) in order to demonstrate the a good agreement between the two.

The mean offset is  $+0.51 \pm 0.66$  km/s (sdom,  $N=31$ ), indicated as a solid line in the lower panel of Figure.4(b), the dotted line indicates a 2 dispersion. Among the 35 stars under consideration, two stars, namely, HD 6755 and BD+17 4708, exhibit velocity differences greater than the 2 dispersion, while HD 8724, HD 165908, and BD+29 366 exhibit the velocity differences close to the 2 dispersion. These are indicated as filled squares in the lower panel of Figure 4(b). BD+17 4708 and HD 6755 are known as binaries in previous radial velocity studies of Latham et al. (2002) and Carney et al. (2003), and our radial velocities are in good agreement with the radial velocity curves calculated from their orbital solutions. HD 165908 is also a star in a binary system (b Her). BD+29 366 is a suspected binary with an unknown period (Latham et al. 2002). Only one previous radial velocity study (Barbier-Brossat 1989) exists in relation to HD 8724. Considering its error of 1 km/s and a velocity difference of approximately 2.5 km/s from our results, we suspect that HD 8724 may be a binary system, which requires further radial-velocity study.

## 3. Atmospheric parameters

In order to derive elemental abundances, an appropriate model atmosphere must be constructed prior to conducting abundance analysis. We used Kurucz model atmosphere grids

computed with the new opacity distribution function (ODF) (<http://kurucz.harvard.edu>). A Linux ported ATLAS program (Sbordone et al. 2004) was used to interpolate model atmospheres for the atmospheric model between grid points. For the metal-poor stars with  $[Fe/H] < -0.5$ ,  $\alpha$ -element enhanced models ( $[Fe/H] = +0.4$ ) were used. The adopted  $\log g$  values for the iron lines are presented in Table 2. For the determination of atmospheric parameters, we used only the Fe I and Fe II lines weaker than  $\log(EW/\text{\AA}) < 4.90$  or  $EW < 100\text{m\AA}$  in order to avoid the saturated lines. The LTE abundance analysis program, MOOG, (Snedden 1973) was used to derive Fe I and Fe II abundances.

We determined the atmospheric parameters by following a self-consistent LTE analysis technique. First, the value of  $T_e$  was adjusted so that there is no trend between the iron abundances from each of the Fe I lines and their lower level excitation potentials. The micro-turbulent velocity ( $v_t$ ) was then determined to exhibit no correlation with the Fe I line strength and the iron abundance derived from each lines. Finally, the value of  $\log g$  was adjusted so that the iron abundance derived from the Fe I lines matches the iron abundance given from the Fe II lines. This process was iterated until the determined parameters ( $T_e$ ,  $\log g$ , and  $v_t$ ) satisfied the above criteria simultaneously. We used more than 100 Fe I lines and a few tens of Fe II lines to determine the atmospheric parameters. Figure. 5 shows the Fe abundance of HD 122563 with the optimal atmospheric parameters to be set as  $T_e = 4430\text{K}$ ,  $\log g = 0.58$ ,  $v_t = 2.15\text{km/s}$ , and  $\log F_{Fe} = 4.68$ . The derived atmospheric parameters derived for our program stars are presented in Table 4.

We compared the atmospheric parameters derived in our study with those obtained in other studies for common objects. This is depicted in Figure 6, where each symbol represents a comparison of our atmospheric parameters with those obtained in other literature, using the following key. A filled square represents comparison with Gratton & Ortolani (1984), a plus symbol indicates comparison with Sneden, Gratton, & Crocker (1991), open square, Gratton & Sneden (1994), open circle, Fulbright (2000), filled triangle, Mishenina & Kovtyukh (2001), open triangle, Gratton et al. (2003), open star, Honda et al. (2004), filled star, Cayrel et al. (2004), and filled circle, Johnsell et al. (2005). We have examined whether a systematic difference exists in the atmospheric parameters depending on the method employed. The atmospheric parameters in Fulbright (2000) were derived in essentially the same manner as in our study, with the exception that the metal abundance of the model atmosphere was enhanced in Fulbright (2000) in order to compensate for the increased electron density caused by  $\alpha$ -element enhancement in metal-poor stars.

As shown in Figure. 6 (a), the effective temperatures obtained in this work are in good agreement with those of other studies. The  $\Delta T_e$  is the mean of  $T_e = T_e$  (this study)  $T_e$  (other studies) between our study and Fulbright (2000), wherein  $T_e$  was de-

tem in ed using the sam e m ethod, is  $+54 \pm 26\text{K}$  (sdom ,  $N=26$ ). The value of  $h T_e$  i for M ishenina & K ovtyukh (2001), wherein  $T_e$  was derived using wing profile tting of  $H$  , is  $+37 \pm 29\text{K}$  (sdom ,  $N=14$ ) and that for Gratton et al. (2003), wherein  $T_e$  was obtained by employing a photometric method using  $(B - V)$  and  $(b - y)$  color index, is  $59 \pm 26\text{K}$  (sdom ,  $N=7$ ). There are no significant differences in  $T_e$  based on the different methods employed. In general, errors of up to  $100\text{K}$  in effective temperature are acceptable.

Figure. 6 (b) shows the comparison of the  $\log g$  values obtained in this study with those obtained in other studies. The mean offset in  $\log g$  is  $+0.08 \pm 0.05$  in the case of Fulbright (2000) and  $+0.11 \pm 0.06$  in M ishenina & K ovtyukh (2001), wherein surface gravity was determined using the ionization balance between Fe I and Fe II lines. In Gratton et al. (2003), surface gravities were obtained using absolute visual magnitudes deduced from Hipparcos parallaxes and masses obtained by interpolating the position of the star along the isochrones. The typical values of their errors in surface gravity, resulting mainly from uncertainties in the parallaxes, is approximately  $0.1$  dex. The mean difference in surface gravities in Gratton et al. (2003) is  $0.08 \pm 0.08$  dex. Thus no significant differences are observed. The non-LTE effect may result in a difference between the surface gravities determined by the photometric method and the spectroscopic method, which is based on the LTE assumption involving ionization balance. This non-LTE effects are expected to be significant under the low surface gravity condition. Comparison of common objects common between this study and Gratton et al. (2003), whose program stars are subdwarfs or early subgiants, shows no significant difference.

Figure. 6 (d) present a comparison of the iron abundance obtained in this study with that obtained in other studies. While Fulbright (2000) used the same method for deriving atmospheric parameters, the value of  $[\text{Fe}/\text{H}]$  in the atmospheric model used in Fulbright (2000) was set marginally higher than the derived iron abundance in order to compensate for the electron density due to  $\alpha$ -elements enhancement in metal-poor stars. Using an  $\alpha$ -enhanced ( $+0.4$  dex) model in our study, we compared the  $[\text{Fe}/\text{H}]$  value of our model to that of Fulbright (2000) and observed no difference ( $0.00 \pm 0.02$  dex). There are no significant systematic errors in  $[\text{Fe}/\text{H}]$ , however, our results are metal deficient by  $0.06 \pm 0.03$  dex as compared to Gratton et al. (2003), and by  $0.10 \pm 0.03$  dex as compared to M ishenina & K ovtyukh (2001).

#### 4. Summary

We have obtained high-resolution ( $R \sim 30\text{k}$ ), high signal-to-noise ( $S/N \sim 100$ ) spectra of 35 metal-poor stars using the BOES at BOAO, with a wavelength range of  $3,800$  to  $10,500\text{\AA}$ .



EW s were measured using the Gaussian fitting method, and the local continuum for each line was determined by visual inspection. In cases where only strong lines were available for a given element, EW s were measured by the Voigt profile fitting method. Thus, we presented the EW s of various elements. The measured EW s are in strong agreement with those of previous studies.

Radial velocities were determined with an error of  $\pm 0.45$  km/s from the Fe lines that were isolated and well-defined as Gaussian profiles. HD 8724 is suspected to be a binary system. The atmospheric parameters were determined by following a self-consistent LTE analysis technique.

$T_e$  was chosen such that Fe I lines of different excitation potentials yield the same abundance and surface gravity was determined from the ionization balance of Fe I and Fe II. The micro-turbulent velocity was set to exhibit no correlation between Fe abundance and the strength of the Fe I line. Model atmospheres were constructed using Kurucz LTE atmospheric model calculated with the new ODF. The atmospheric parameters we obtained are in good agreement with those of previous studies despite the other studies adapting methods different from ours to obtain these parameters.

## REFERENCES

- Aoki, W. et al. 2005, *ApJ*, 632, 611
- Barbier-Brosat, M. 1989, *A & A S*, 80, 67
- Bard, A., Kock, M. 1994, *A & A*, 282, 1014
- Bard, A., Kock, A., & Kock, M. 1991, *A & A*, 248, 315
- Bielsky, A. 1975, *J. Quant. Spectrosc. Radiat. Transfer*, 15, 463
- Biemont, E., Hibbert, A., Godefroid, M., Vaek, N., & Fawcett, B. C. 1991a, *ApJ*, 375, 818
- Biemont, E., Baudoux, M., Kurucz, R. L., Ansbacher, W., & Pinnington, E. H. 1991b, *A & A*, 249, 539
- Biemont, E., Grevesse, N., Hannaford, P., & Lowe, R. M. 1981, *ApJ*, 248, 867
- Bizzarri, A., Huber, M. C. E., Noels, A., Grevesse, N., Bergeson, S. D., Tsekris, P., & Lawler, J. E. 1993, *A & A*, 273, 707
- Blackwell, D. E., Shallis, M. J., & Simmons, G. J. 1980, *A & A*, 81, 340

- Booth, A . J ., Blackwell, D . E ., Petford, A . D ., & Shallis, M . J . 1984, MNRAS, 208, 435
- Burris, D . L ., Pilachowski, C . A ., Arm andro , T . A ., Sneden, C ., Cowan, J . J ., & Roe, H .  
2000, ApJ, 544, 302
- Cardon, B . L ., Sm ith, P . L ., Scalb, J . M ., & Testern an, L . 1982,
- Camey, B . W ., Latham , D . W ., Stefanik, R . P ., Laird, J . B ., & M orse, J . A . 2003, AJ, 125,  
293
- Cayrel, R . et al. 2004, A & A , 416, 1117
- Chiosi, C ., Bertelli, G ., & Bressan, A . 1992, ARAA , 30, 235
- Den Hartog, E . A ., Law ler, J . E ., Sneden, C ., & Cowan, J . J . 2006, ApJ, 167, 292
- Den Hartog, E . A ., Law ler, J . E ., Sneden, C ., & Cowan, J . J . 2003, ApJS, 148, 543
- Fischer, C . F . 2002, <http://www.vuse.vanderbilt.edu/~c>
- Fields, B . D ., Truran, J . W ., & Cowan, J . J . 2002, ApJ, 575, 845
- Francois, P . et al. 2007, A & A , 476, 935
- Fulbright, J . P . 2000, AJ, 120, 1841
- G ilroy, K . K ., Sneden, C ., Pilachowski, C . A ., & Cowan, J . J . 1988, ApJ, 327, 298
- G ratton, R . G . & Ortolani, S . 1984, A & A , 137, 6
- G ratton, R . G . & Sneden, C . 1994, A & A , 287, 927
- G ratton, R . G . et al. 2003, A & A , 404, 187
- Hannaford, P ., Lowe, R . M ., G revesse, N ., & Noels, A . 1992, A & A , 259, 301
- Hannaford, P ., Lowe, R . M ., G revesse, N ., B iem ont, E ., & W haling, W . 1982, ApJ, 261, 736
- Holweger, H ., Heise, C ., & Kock, M . 1990, A & A , 232, 510
- Honda, S . et al. 2004, ApJ, 607, 474
- Johnsell, K . et al. 2005, A & A , 440, 321
- K in , K . M ., et al. 2002, JKAS, 35, 221
- Kunucz, R . L . 1995, Kunucz CD -ROM No 23 (Harvard-Sm ithsonian Center for Astrophysics)

- Kupka, F., Piskunov, N. E., Ryabchikova, T. A., Stenples, H. C., & Weiss, W. W. 1999, *A & A S*, 138, 119
- Kusz, J. 1992, *A & A S*, 92, 517
- Latham, D. W. et al. 2002, *A J*, 124, 1144
- Lawler, J. E., Bonvallet, G., & Sneden, C. 2001a, *ApJ*, 556, 452
- Lawler, J. E., Wickliffe, M. E., Cowley, C. R., & Sneden, C. 2001b, *ApJS*, 137, 341
- Lawler, J. E., Den Hartog, E. A., Labby, Z. E., Sneden, C., Cowan, J. J. and Ivans, I. I. 2007, *ApJS*, 169, 120
- Lawler, J. E., Den Hartog, E. A., Sneden, C., & Cowan, J. J. 2006, *ApJS*, 162, 227
- Matteucci, F. 2001, *The Chemical Evolution of the Galaxy*, Kluwer Academic Publishers, Dordrecht
- McWilliam, A., Preston, G. W., Sneden, C., & Searle, L. 1995, *A J*, 109, 2757
- McWilliam, A. 1998, *A J*, 115, 1640
- Mendoza, C., Eissner, W., Zeppen, C. J., & Galavis, M. E. 1995, <http://legacy.nasa.gov/topbase>
- Mishenina, T. V. & Kovtyukh, V. V. 2001, *A & A*, 370, 951
- Montes, F., Beers, T. C., Cowan, J., Elliot, T., Farouqi, K., Gallino, R., Heil, M., Kratz, K.-L., Pfeifer, B., Pignatari, M., & Schatz, H. 2007, 671, 1685
- Nordstrom, B. et al. 2004, *A & A*, 418, 989
- O'Brien, T. R. & Lawler, J. E. 1991a, *Phys. Rev. A*, 44, 7134
- O'Brien, T. R., Wickliffe, M. E., Lawler, J. E., Whaling, J. W. & Brault, W. 1991b, *JO SA B*, 9, 1185
- Pagel, B. E. J. 1997, *Nucleosynthesis and Chemical Evolution of Galaxies* (Cambridge Univ. Press)
- Palmieri, P., Quinet, P., Wyard, J.-F., & Biemont, E. 2000, *Phys. Scr.*, 61, 323
- Ryan, S. G., Norris, J. E., & Beers, T. C. 1996, *ApJ*, 471, 254

- Sbordone, L., Bonifacio, P., Castelli, F., & Kurucz, R. L. 2004, *M S A I S*, 5, 93
- Smith, G., & Raggett, S. St. J. 1981, *Phys. Rev. B*, 14, 4015
- Snedden, C. 1973, *A p J*, 184, 839
- Snedden, C., Gratton, R. G., & Crocker, D. A. 1991, *A & A*, 246, 354
- Tinsley, B. M. 1980, *Fundamentals of Cosmic Physics Vol 5*, p 287
- Turan, J. W., Cowan, J. J., Pilachowski, C. A., & Sneden, C. 2002, *P A S P*, 114, 1293
- Weiss, A. W. 1963, *A p J*, 138, 1262
- Heeler, J. C., Sneden, C., & Turan, J. W. 1989, *A R A A*, 27, 279

Table 1. Observational Log

Num .	Object	R A .(J2000)	Dec.(J2000)	V	Observation date	t <sub>exp</sub>	S=N
1	HD 2665	00 30 45:44	+ 57 03 53:6	7.65	Nov. 2005	1800	250
2	HD 6755	01 09 43:00	+ 61 32 30:2	7.68	Nov. 2005	1800	250
3	HD 8724	01 26 17:59	+ 17 07 35:1	8.30	Nov. 2005	2000	250
4	BD + 29 0366	02 10 24:50	+ 29 48 23:7	8.79	Nov. 2005	2400	240
5	HD 19445	03 08 25:58	+ 26 19 51:4	8.04	Nov. 2005	2400	260
6	HD 21581	03 28 54:49	00 25 03:1	8.70	Nov. 2005	2400	220
7	HD 25532	04 04 11:01	+ 23 24 27:1	8.18	Nov. 2005	2400	220
8	HD 29587	04 41 36:32	+ 42 07 06:5	7.28	Nov. 2005	2400	300
9	BD + 37 1458	06 16 01:52	+ 37 43 18:7	8.92	Nov. 2005	2400	160
10	HD 45391	06 28 46:03	+ 36 28 47:9	7.11	Nov. 2005	2400	280
11	HD 58551	07 26 50:25	+ 21 32 08:3	6.53	Nov. 2005	600	300
12	HD 59374	07 30 29:02	+ 18 57 40:6	8.51	Nov. 2005	3000	230
13	HD 64090	07 53 33:12	+ 30 36 18:2	8.27	Nov. 2005	3600	250
14	HD 63791	07 54 28:70	+ 62 08 10:8	8.20	Nov. 2005	3600	250
15	HD 73394	08 40 22:54	+ 51 45 06:6	7.71	Apr. 2006	2400	150
16	HD 84937	09 48 56:00	+ 13 44 39:3	8.29	Nov. 2005	1800	250
17	HD 237846	09 52 38:68	+ 57 54 58:6	9.94	Nov. 2005	7200	200
18	HD 93487	10 47 55:53	+ 23 20 07:0	7.71	Apr. 2006	4800	130
19	HD 94028	10 51 28:12	+ 20 16 39:0	8.23	Apr. 2006	3000	150
20	HD 101227	11 39 06:22	+ 44 18 20:3	8.39	Apr. 2006	4800	175
21	HD 105546	12 09 02:72	+ 59 01 05:1	8.61	Apr. 2006	3600	130
22	HD 114095	13 08 25:79	07 18 30:5	8.35	Apr. 2006	4000	120
23	HD 114762	13 12 19:74	+ 17 31 01:6	7.30	Apr. 2006	2400	170
24	HD 118659	13 38 00:47	+ 19 08 53:1	8.84	Apr. 2006	4800	110
25	HD 122563	14 02 31:85	+ 09 41 09:9	6.20	Apr. 2006	1800	220
26	HD 123710	14 04 57:07	+ 74 34 24:9	8.21	Apr. 2006	3600	160
27	HD 148816	16 30 28:46	+ 04 10 41:0	7.27	Apr. 2006	3000	110
28	HD 159482	17 34 43:06	+ 06 00 51:6	8.39	Apr. 2006	4800	160
29	HD 165908	18 07 01:54	+ 30 33 43:7	5.07	Apr. 2006	300	200
30	HD 175305	18 47 06:44	+ 74 43 31:4	7.20	Apr. 2006	2400	260
31	HD 201889	21 11 59:52	+ 24 10 05:0	8.04	Nov. 2005	1800	240
32	HD 204543	21 29 28:21	03 30 55:4	8.31	Nov. 2005	2400	290
33	BD + 22 4454	21 39 36:46	+ 23 15 55:9	9.50	Nov. 2005	1800	140
34	BD + 17 4708	22 11 31:37	+ 18 05 34:2	9.47	Nov. 2005	5400	120
35	HD 221170	23 29 28:81	+ 30 25 57:8	7.71	Nov. 2005	1200	260

{ 14 {

Table 2. Equivalent Widths

Wavelength	Species	eV	log gf	Equivalent Width (mÅ)										
				1	2	3	4	5	6	7	8	9	10	11
6335.34	Fe I	2.20	-2.27	51.2	67.4	90.9	61.9	10.2	73.7	61.0	78.3	25.7	80.6	62.9
6380.75	Fe I	4.19	-1.37	3.7	9.7	16.8	15.8		12.6	11.5	30.1		33.3	20.7
6392.54	Fe I	2.28	-3.97		3.8	7.4	3.8		3.5		6.6		7.4	
6393.61	Fe I	2.43	-1.43	73.6	85.9	108.4	85.3	23.4	92.6	88.4	106.4	45.6	111.9	85.4
6411.66	Fe I	3.65	-0.60	41.2	61.7	78.8	74.5	12	68.1	65.8	102.4	27.5	109.8	79.0
6421.36	Fe I	2.28	-2.03	58.2	74.0	98.8	70.3	13.7	83.5	76.5	90.5	33.1	93.4	73.9
6481.88	Fe I	2.28	-2.98	15.8	33.4	50	23.3		32.9	28.6	50.8	8.9	47.0	24.0
6498.94	Fe I	0.96	-4.70	38.5	17.8	42.2	13.5	13.8	24.6	11.1	26.8		28.3	9.2
6518.37	Fe I	2.83	-2.46	7.2	18.5	30.9	24.5	1.8	23.8	19.5	38.7	3.4	39.3	20.5
6533.94	Fe I	4.56	-1.29	3.9		8.2	6.6		6.3	6.9	18.2		20.0	14.5
6574.25	Fe I	0.99	-5.00	6.2		36.8			14.6		15.8		16.1	
6581.22	Fe I	1.49	-4.68			14	5		7.4	4.2	10.2		11.0	4.2
6593.88	Fe I	2.43	-2.42	31.9	43.9	68.8	44.3		53.4	37.6	63.1	11.5	66.9	45.2
6608.04	Fe I	2.28	-3.96		3.1		3.1		4.6		7.1		8.7	3.4
6609.12	Fe I	2.56	-2.69	12.6	24.9	43.4	24.7		32.2	18.4	43.9		47.2	26.1
6625.04	Fe I	1.01	-5.37		3.4	10.5	5.1		7.7		7.9		9.5	
6627.56	Fe I	4.55	-1.50		4.0	2.9	4		3.4		12.0		12.4	8.5
6633.76	Fe I	4.56	-0.82	6.9	11.7		23.6	2.3	15.5	15.5	41.1		44.8	29.6
6703.58	Fe I	2.76	-3.01	3.9	8.5	14.9	7.9		10.3	5.7	18.8		19.5	8.4
6713.75	Fe I	4.80	-1.41			2.5	2.2		4.4		9.2		9.4	5.4

Note. | Table 2 is presented in its entirety in the electronic edition of the Astrophysical Journal. A portion is shown here for guidance regarding its form and content.

Table 3. References of adopted log gf value

Species	Reference	Species	Reference
Fe I	Oxford group	V I	VALD (Kupka et al. 1999)
	Bard et al. (1991)	V II	VALD (Kupka et al. 1999)
	Bard & Kock (1994)	Cr I	Oxford group
	O'Brien et al. (1991)	Mn I	Booth et al. (1984)
Fe II	Holweger et al. (1990)	Co I	Cardon et al. (1982)
	Bienont et al. (1991b)	Ni I	VALD (Kupka et al. 1999)
	Hannaford et al. (1992)	Cu I	Bielsky (1975)
	Blackwell et al. (1980)	Zn I	VALD (Kupka et al. 1999)
Li I	Weiss (1963)	Sr II	Gratton & Sneden (1994)
O I	Bienont et al. (1991a)	Y II	Hannaford et al. (1982)
Ø I	Kurucz (1995)	Zr II	Bienont et al. (1981)
Na I	Fischer (2002)	Ba II	McWilliam (1998)
Mg I	Gratton et al. (2003)	La II	Lawler et al. (2001a)
Al I	Mendoza et al. (1995)	Ce II	Palmer et al. (2000)
Si I	O'Brien & Lawler (1991)	Nd II	Den Hartog et al. (2003)
K I	NIST	Sm II	Lawler et al. (2006)
Ca I	Smith & Raggett (1981)	Eu II	Lawler et al. (2001b)
Sc II	NIST	Dy II	Kusz (1992)
Ti I	Oxford group	Hf II	Lawler et al. (2007)
Ti II	Bizzarri et al. (1993)		



Table 4. Atmospheric parameters and radial velocities of stars

Num	ID	T <sub>e</sub>	log g	v	log "Fe	[Fe/H]	V <sub>rad</sub>
1	HD 2665	4770	1.65	1.55	5.26	2.26	382.68 0.44
2	HD 6755	5050	2.58	1.23	5.88	1.64	312.55 0.42
3	HD 8724	4720	1.65	1.57	5.84	1.68	113.76 0.45
4	BD+ 29 0366	5640	4.35	0.75	6.48	1.04	26.91 0.33
5	HD 19445	5825	4.20	0.50	5.34	2.18	140.11 0.50
6	HD 21581	4920	2.29	1.30	5.88	1.64	153.04 0.37
7	HD 25532	5570	2.34	2.10	6.26	1.26	111.73 0.48
8	HD 29587	5670	4.43	1.08	6.89	0.63	112.59 0.38
9	BD+ 37 1458	5240	3.14	1.00	5.31	2.21	242.60 0.38
10	HD 45391	5720	4.50	1.05	7.00	0.52	5.15 0.43
11	HD 58551	6270	4.28	1.41	6.97	0.55	51.21 0.45
12	HD 59374	5800	4.24	0.83	6.54	0.98	91.32 0.40
13	HD 64090	5310	4.65	0.60	5.68	1.84	234.22 0.48
14	HD 63791	4750	1.82	1.60	5.81	1.71	107.00 0.41
15	HD 73394	4530	1.48	1.93	5.96	1.56	101.23 0.39
16	HD 84937	6180	3.71	1.00	5.21	2.31	15.02 0.51
17	HD 237846	4680	1.28	1.63	4.40	3.12	303.99 0.39
18	HD 93487	5350	2.45	1.90	6.47	1.05	79.11 0.43
19	HD 94028	5950	4.23	0.80	6.01	1.51	65.44 0.41
20	HD 101227	5550	4.51	0.90	7.10	0.42	11.61 0.34
21	HD 105546	5200	2.23	1.60	6.03	1.49	18.01 0.38
22	HD 114095	4880	2.93	1.40	6.91	0.61	75.82 0.38
23	HD 114762	5950	4.32	1.15	6.74	0.78	49.58 0.39
24	HD 118659	5510	4.50	0.68	6.85	0.67	44.96 0.35
25	HD 122563	4430	0.58	2.15	4.68	2.84	26.27 0.37
26	HD 123710	5750	4.55	0.75	6.98	0.54	13.18 0.34
27	HD 148816	5800	4.13	0.80	6.70	0.82	47.68 0.33
28	HD 159482	5770	4.31	0.83	6.67	0.85	139.94 0.36
29	HD 165908	5970	4.24	1.18	6.89	0.63	1.50 0.33
30	HD 175305	5030	2.52	1.48	6.06	1.46	184.60 0.40
31	HD 201889	5700	4.33	0.95	6.71	0.81	103.22 0.40
32	HD 204543	4720	1.27	2.00	5.73	1.79	98.74 0.39
33	BD+ 22 4454	5150	4.43	0.00	6.98	0.54	106.92 0.35
34	BD+ 17 4708	6060	3.83	0.97	5.80	1.72	296.70 0.49
35	HD 221170	4580	1.32	2.00	5.42	2.10	121.73 0.43

{ 18 {

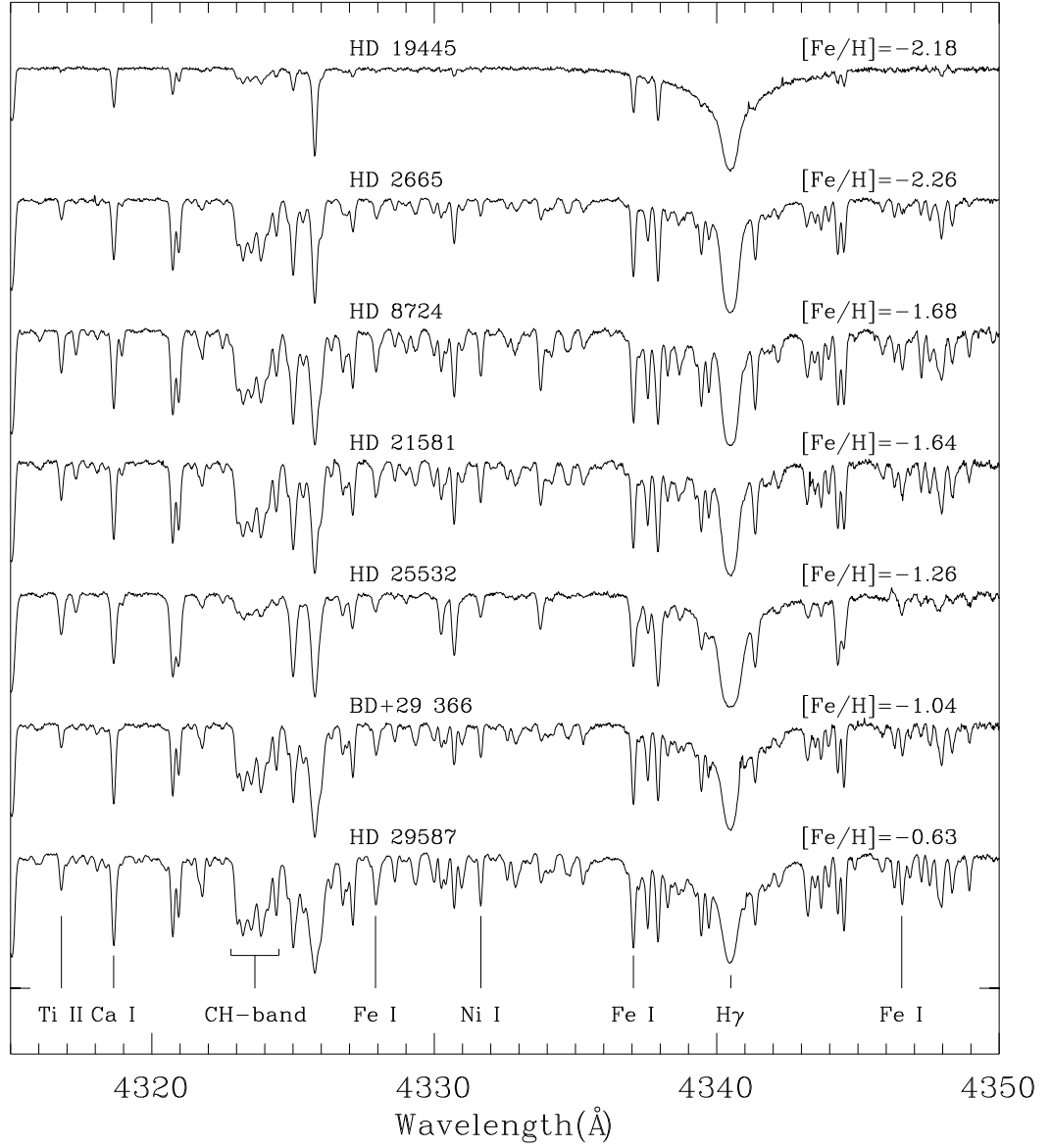


Fig. 1. | Examples of spectra for seven stars over a wavelength range of 4315–4350 Å. Several identified lines are indicated. This spectral region includes the CH molecular band used for deriving carbon abundance. H $\gamma$  line is observed at 4340 Å.

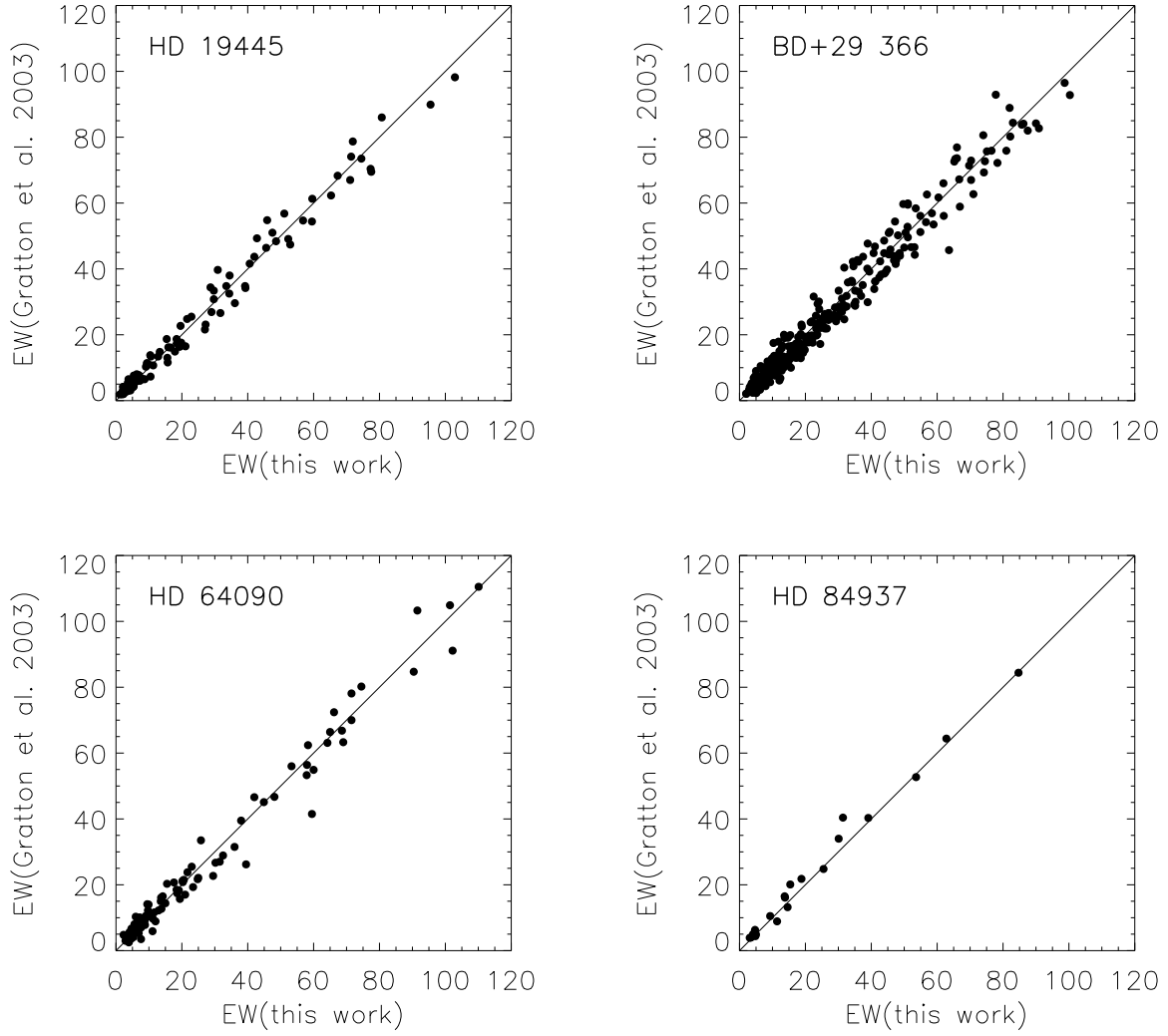


Fig. 2. Comparison between the EW s(in m Å ) measured from the BOES spectra and those corresponding to Gratton et al. (2003)

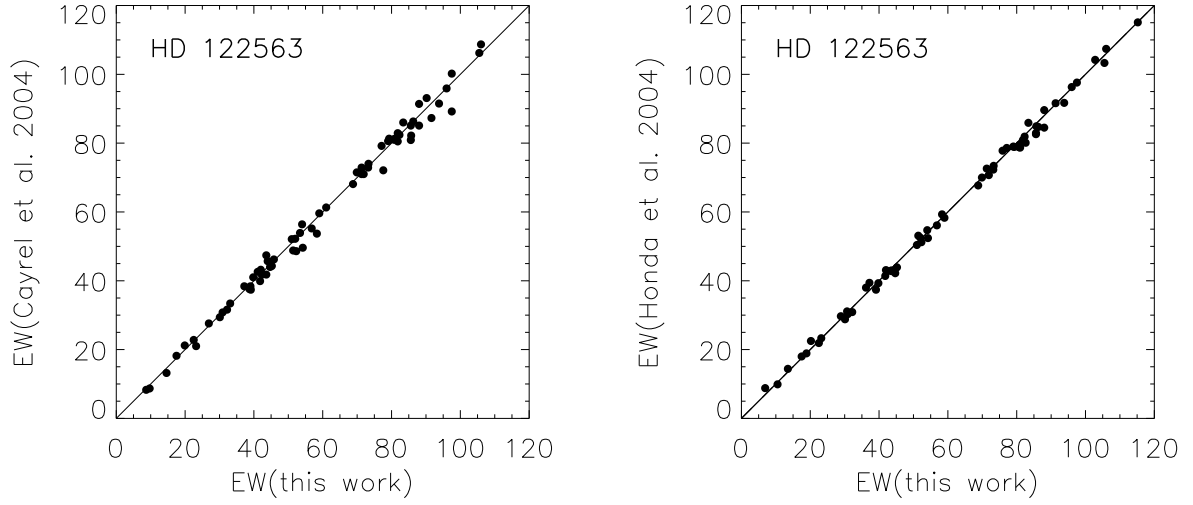


Fig. 3. Comparison between the EW s measured from the BOES spectra and those corresponding to Cayrel et al. (2004) and Honda et al. (2004) for HD 122563

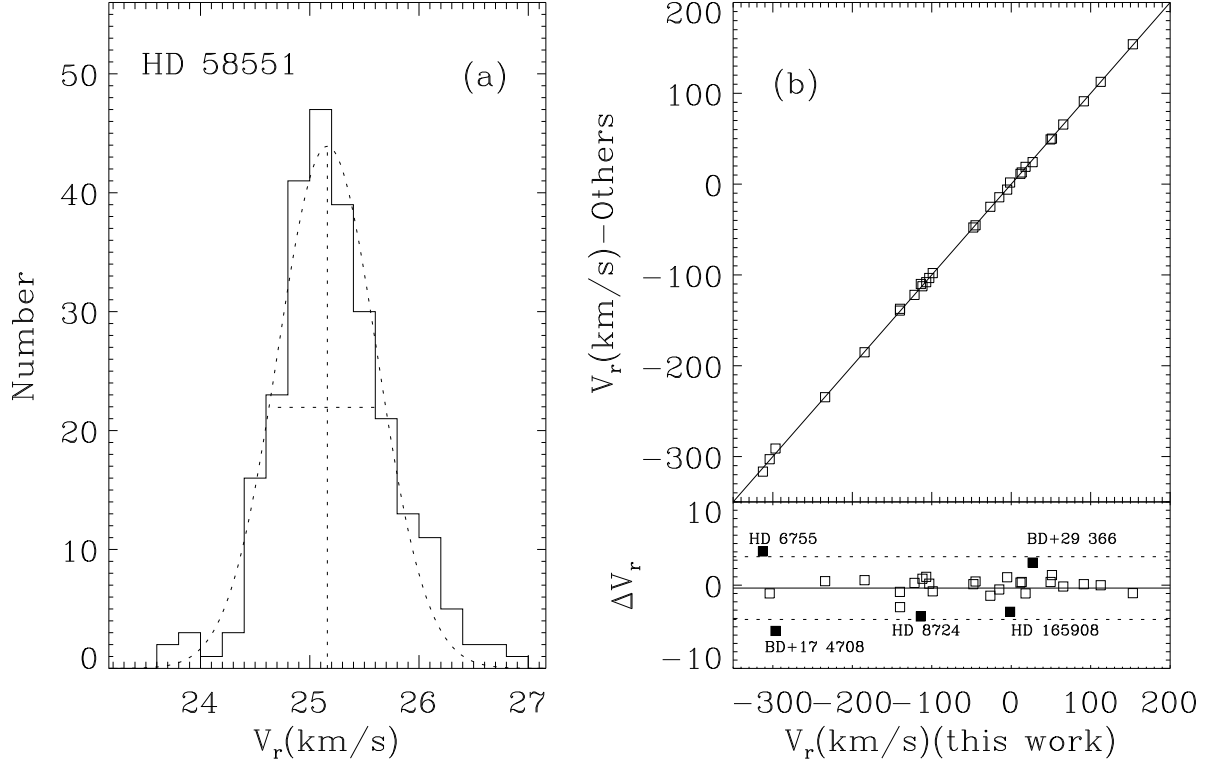


Fig. 4. (a) An example of the determination of radial velocity of HD 58551 prior to heliocentric velocity correction. The dotted line is the Gaussian fitting result. (b) (Upper panel) Comparison between radial velocities measured from the BOES spectra and those from other radial velocity studies. (Lower panel) Differences in radial velocities. The solid line represents the mean of set and the dotted line represents a  $2\sigma$  dispersion of velocity differences. The velocities of HD 6755, HD 8724, HD 165908, and BD+17 4708, represented as filled squares, show large deviations from previous studies. These stars, except HD 8724, are known as binaries.

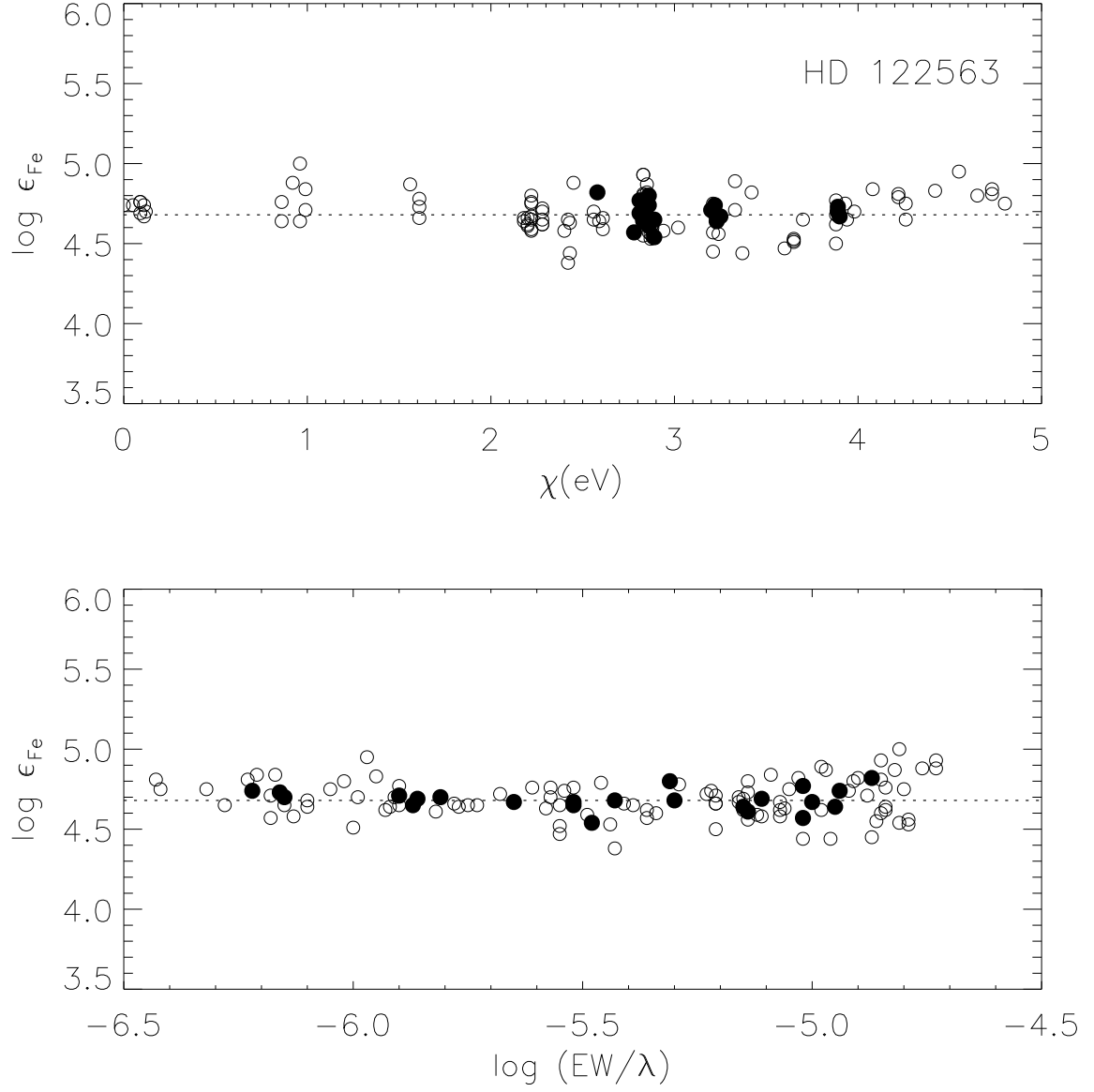


Fig. 5. | Fe abundances for HD 122563 with derived atmospheric parameters ( $T_e = 4430\text{K}$ ,  $\log g = 0.58$ ,  $v_t = 2.15 \text{ km/s}$ ). Open circle shows iron abundance derived from the Fe I line and filled circle shows that derived from the Fe II line.

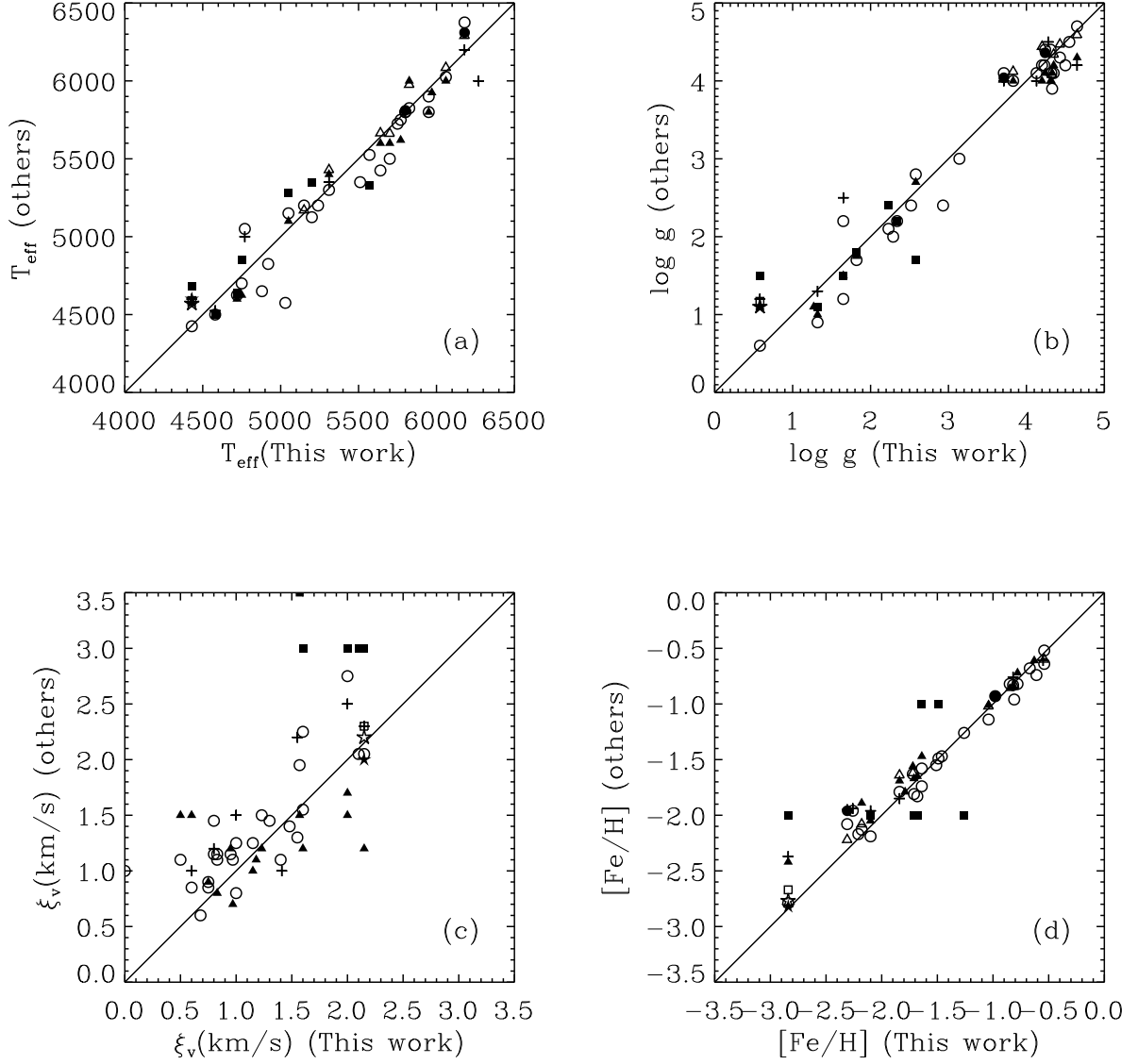


Fig. 6. | Atmospheric parameter ( $T_e$ ,  $\log g$ ,  $\xi_v$ ,  $[\text{Fe}/\text{H}]$ ) comparisons between this study and various other studies. Filled square indicates comparison with Gratton & Ortolani (1984); plus, indicates comparison with Sneden, Gratton, & Crocker (1991); open square, Gratton & Sneden (1994); open circle, Fulbright (2000); filled triangle, Mishenina & Kovtyukh (2001); open triangle, Gratton et al. (2003); open star, Honda et al. (2004); filled star, Cayrel et al. (2004); and filled circle, Johnson et al. (2005)